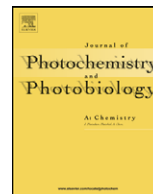




Contents lists available at ScienceDirect

# Journal of Photochemistry and Photobiology A: Chemistry

journal homepage: [www.elsevier.com/locate/jphotochem](http://www.elsevier.com/locate/jphotochem)

## Inactivation of *E. coli* mediated by high surface area CuO accelerated by light irradiation >360 nm

M. Paschoalino<sup>a</sup>, N.C. Guedes<sup>a</sup>, W. Jardim<sup>a,\*\*</sup>, E. Mielczarski<sup>b</sup>,  
J.A. Mielczarski<sup>b</sup>, P. Bowen<sup>c</sup>, J. Kiwi<sup>d,\*</sup>

<sup>a</sup> Institute of Chemistry, UNICAMP, State University of Campinas, Campinas, Brazil

<sup>b</sup> INPL/CNRS, UMR 7569 LEM, 15 Av du Charmois, 54501 Vandoeuvre les Nancy, France

<sup>c</sup> Laboratory of Powder Technology, Institute of Materials, Station 12, Swiss Federal Institute of Technology (EPFL) Lausanne 1015, Switzerland

<sup>d</sup> Laboratory of Chemical Reaction Engineering LGRC, Station 6, Swiss Federal Institute of Technology (EPFL) Lausanne 1015, Switzerland

### ARTICLE INFO

#### Article history:

Received 12 February 2008

Received in revised form 24 April 2008

Accepted 5 May 2008

Available online 15 May 2008

#### Keywords:

High BET CuO

*E. coli*

Photocatalysis

Bacterial immobilization

XPS

### ABSTRACT

CuO powders with different specific surface areas are reported hereby to inactivate *E. coli* in aqueous solution in the dark under visible light irradiation  $\lambda > 360$  nm. The inactivation of *E. coli* mediated by the CuO suspensions was investigated as a function of the solution parameters: specific surface area of the Cu-oxides (40–77 m<sup>2</sup>/g), amount of CuO, light intensity and fate of the Cu<sup>1+</sup>-ion within the inactivation process. The specific surface area of the CuO was observed to play an important role during the *E. coli* inactivation kinetics. The light induced inactivation of *E. coli* in CuO suspensions (1 g/L) was complete within 4 h. The cytotoxicity of *E. coli* when using CuO (77 m<sup>2</sup>/g) was found for CuO concentrations as low as 0.2 g/L. A reaction mechanism is suggested for the Fenton-like reactions due to the Cu-ions/CuO action and the reactive oxygen species (ROS) generated in solution. These highly oxidative radicals decompose Orange II and methylene blue (MB) dyes in aqueous solution of CuO. The CuO in contact with the bacterial suspension shows a change in its surface oxidation state from Cu<sup>2+</sup> to Cu<sup>1+</sup>. The outermost layer of the catalyst (5–7 nm) becomes mainly Cu<sub>2</sub>O (80%) and CuO (20%) as observed by X-ray photoelectron spectroscopy (XPS). A shift of the Cu 2p<sub>3/2</sub> peak from the initial position at 933.6–932.6 eV upon contact of the *E. coli* with CuO was observed concomitant with the disappearance of the Cu<sup>2+</sup> shake-up satellite lines at 942.3 and 962.2 eV. The XPS surface composition of copper catalyst is reported at different stages of *E. coli* inactivation and it was observed that the reduced copper oxide remains stable during the 4 h needed to inactivate the *E. coli* suspension.

© 2008 Elsevier B.V. All rights reserved.

### 1. Introduction

Reactions involving Cu<sup>1+</sup>/Cu<sup>2+</sup> leading to the oxidative transformations of organic compounds have been discussed recently in some reviews [1,2]. The unique electronic structure of Cu allows the interaction with the spin restricted O<sub>2</sub>, enabling Cu to participate as in redox reactions with inorganic and organic compounds. The Cu-oxalate has been reported to decompose partially upon heating into a low valence state (Cu(I)) as reported in a previous study by our laboratory [3] but then oxidizes back to Cu(II) in solution when using as a photocatalyst [3,4]. Recently, the favorable activity of large surface area CuO leading to the oxidative photodegradation of phenols was reported [5]. In the present study, we will show that

the photocatalytic activity of the CuO powders under light irradiation lead to the degradation of the anionic dye Orange II [5] and the cationic dye methylene blue (MB) [6,7]. CuO has been used as heterogeneous catalyst leading to the degradation of N<sub>2</sub>O, the reduction of NO to NH<sub>3</sub> [8,9] and the catalytic oxidation of different phenols [10]. Some preparations of ultrafine particles of CuO have been carried out by precipitation [11], freeze-dry [12] and the sol-gel route [13].

The objective of this study was to explore large surface area CuO powders obtained by Cu-oxalate decomposition [3] applied to the inactivation of *E. coli* in aqueous suspension due to the bactericide properties of CuO. Work with nanoparticulate CuO is warranted since CuO is beginning to be used as an external disinfecting agent for skin treatment with encouraging results. We will also show that CuO mediates the photodegradation of Orange II and MB, due to the highly oxidative radicals produced by CuO in aqueous solution. This makes CuO a useful bactericide besides being a photocatalyst able to degrade organic compounds.

\* Corresponding author.

\*\* Corresponding author.

E-mail address: [john.kiwi@epfl.ch](mailto:john.kiwi@epfl.ch) (J. Kiwi).

## 2. Experimental

### 2.1. Materials

Cu-nitrate hydrated, Na-oxalate, and hydroxy-propyl-methyl cellulose (HPMC),  $H_2O_2$ , CuO, Orange II, MB KI, K-phthalate, NaOH, hexa-ammonium molybdate hexahydrate were Aldrich p.a. reagents and used as received. Tri-distilled water was used throughout this study.

### 2.2. Synthesis of high surface area CuO

The synthesis of the CuO was carried out in a tubular furnace under controlled air flow (Sorvall–Heraeus) by thermal decomposition of Cu-oxalate was carried as reported [3]. Other salts of Cu were explored and did not lead to CuO with higher specific area or activity since the Cu-source seems to influence the crystal growth of the CuO building units.

### 2.3. Irradiation procedures and analyses

A Columed (150 W) mercury lamp was used as shown in Fig. 1 with a cutoff filter for wavelengths with  $\lambda \leq 360$  nm (see insert with Fig. 1). The filter was a commercial light yellow transparent polyacrylate Plate 3 mm thick. The filter is used to preclude light absorption by *E. coli* membrane bilayer reaching up to 340 nm [14]. This lamp irradiated cylindrical Pyrex photo-reactor (70 mL) containing 40 mL the CuO photocatalyst in the *E. coli* suspensions. The integral radiant flux of the incident light was measured with a power-meter (Newport 1830-C USA) and grey neutral filters were used to monitor the light flux in the experiments where the intensity was varied from 2.4 to 29.2 mW/cm<sup>2</sup>.

Photometric determination of  $H_2O_2$  in solution was carried out using the peroxidase (Aldrich) catalyzed oxidation of *n,n*-diethyl-*p*-phenylenediamine (DPD, from Sigma) with hydrogen peroxide measured at  $\lambda = 551$  nm [15]. The suspensions were filtered with filters (0.20  $\mu$ m) before each analysis to separate the solid from the liquid and the copper interference was precluded using triethylenetetramine (Fluka) complexing agent [16].

The determination of the total amount of  $Cu^{1+}$ -ions in solution was carried out with the neocuproin reagent [3,4]. The Cu-neocuproin complex formed is soluble in chloroform. The absorbance of the complex peak at  $\lambda = 457$  nm was measured

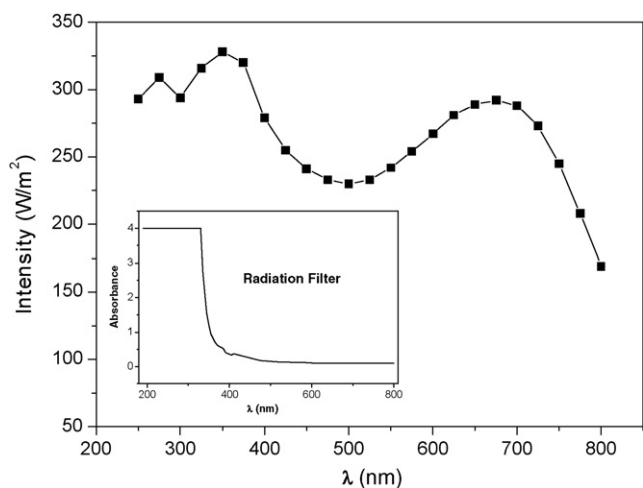


Fig. 1. Spectral distribution of the mercury lamp (150 W) used as irradiation source used in this study to irradiate the suspensions containing *E. coli* and CuO powders. The insert shows the filter used for the UV-component.

against a blank made out of reagents used in the sample in the absence of copper. The absorption peak of the Orange II and MB dyes were followed in a JENWAY 6405 spectrophotometer and the total organic carbon (TOC) decrease occurring concomitantly during the degradation of the dyes was measured with a Shimadzu V-CPN TOC analyzer.

### 2.4. Nitrogen adsorption/desorption measurements

The specific surface area measurements were made by  $N_2$  absorption and the results modeled after the Brunauer–Emmett–Teller (BET) treatment with a Micromeritics Gemini 2375 instrument. Prior to the measurements the powder was dried under  $N_2$  flow at 110 °C for 1 h. The sample was then out-gassed under high vacuum. Full isotherms were collected in a Micromeritics ASAP 2000 instrument and the pore size distribution calculated from the desorption branch following the well known BJH model.

### 2.5. Electrophoresis mobility

The mobility was measured by a Triga Mark II electrophoresis unit of Rank Bros, Cambridge UK. The ZPC of CuO was found to be in a narrow range for the different specific surface area Cu-oxides with values around  $7.4 \pm 0.3$ . To obtain the electrophoresis data the dispersions were left at each pH to stabilize for 2 h. This was necessary since the electrophoretic mobilities should reflect precisely the adsorption capacity of the photocatalyst at a given pH.

### 2.6. X-ray photoelectron spectroscopy (XPS)

AXIS NOVA photoelectron spectrometer (Kratos Analytical, Manchester, UK) equipped with monochromatic Al  $K\alpha$  ( $h\nu = 1486.6$  eV) anode was used in the studies. The kinetic energy of the photoelectrons was determined with the hemispheric analyser set to the pass energy of 160 eV for wide scan spectra and 20 eV for taking the high-resolution spectra. Electrostatic charge effect of sample was overcompensated by means of the low-energy electron source working in combination with the magnetic immersion lens. The carbon C1s line with position at 284.6 eV was used as a reference to correct the charging effect. Quantitative elemental compositions were determined from peak areas using experimentally determined sensitivity factors and spectrometer transmission function.

The Relative Sensitivity Factor (RSF) is the sensitivity of the spectral line to the excitation process (e.g. photon bombardment) relative to F1s peak. The most known RSF is Scofield theoretically calculated RSF and Wagner experimental RSF. Also the Surface and microanalysis NMP816 (DIN) norms were used. The spectrum background was subtracted according to Shirley. The XPS results were corrected by subtracting the background noise and considering the sensitivity factors (RSF) for each element. The high-resolution spectra were analyzed using the deconvolution software Vision 2, Kratos Analytical, UK.

Prior to the XPS analysis of the different samples, the culture medium containing both *E. coli* and CuO were dried at 60 °C in the oven. Therefore, small deposits due to the preparative solution used remained on the catalyst surface. Table 1 shows the elements found in the XPS spectrum coming from *E. coli* decomposition intermediates and from the culture medium.

#### 2.6.1. Evaluation of the bactericidal activity of the CuO samples

The procedure used to monitor the degradation consisted in the preparation of an *E. coli* (*Escherichia coli*–CCT 1457) was in a LB culture medium. The medium used for bacterial growth and evaluation

**Table 1**  
Atomic surface composition in (%)

Surface composition in (%) area of the elements	Cu	O	C	Na	K	P	S
CuO after preparation	24.0	33.0	43.0	–	–	–	–
CuO after contact with bacteria in buffer	0.9	36.9	42.8	3.0	9.4	6.1	0.8

of the biocide activity was glucose minimal salt medium (GMM) when adding 20 g of glucose (D-glucose monohydrated), 3 g of  $K_2HPO_4$ , 7 g of  $KH_2PO_4$ , 1 g of  $(NH_4)_2SO_4$ , 0.5 g of sodium citrate and 0.1 g of  $MgSO_4 \cdot 7H_2O$  to 1 L of distilled water. The pH of the medium was adjusted to 7.1 using NaOH 1 mol/L. All experiments were conducted using a water bath at 37 °C. Aliquots of the overnight culture medium were inoculated into a fresh medium and incubated aerobically at 37 °C until the absorbance value measured at  $\lambda = 550$  nm reached  $\sim 0.05$ , which corresponds to  $10^6$ – $10^8$  CFU/mL, in accordance to the McFarland Scale [17]. After this, CuO was added to the samples at concentrations from 0.1 to 2 g/L. An aliquot of 400  $\mu$ L of the samples were deposited on agar PCA (Plate Count Agar) plates after different reaction times.

### 3. Results and discussion

#### 3.1. Solution parameters for the bacterial inactivation by high surface area CuO

Fig. 2a shows the results of the *E. coli* viability by CuO particulate in the dark. It is seen that within 17 h the *E. coli* decreases from a concentration of  $10^6$  CFU/mL to the limit of the CFU experimental detection, in this case 1 CFU/0.4 mL = 2.5 CFU/mL. The CuO dispersions in the dark in contact with *E. coli* lead to the abatement of *E. coli*. Soluble bactericidal and fungicidal Cu-compounds are used in paints rendering the wood and plastics surfaces self-disinfecting [18].

Fig. 2b shows that in the absence of CuO or in the presence of commercial CuO (0.3–0.5  $m^2/g$ ) a negligible inactivation of *E. coli* takes place. It is readily seen in Fig. 2b that the inactivation of *E. coli* is more efficient as the specific surface area of the CuO increases. No *E. coli* were observed in the CuO suspensions after 4 h illumination for CuO (40–77  $m^2/g$ ) under light ( $h\nu > 360$  nm). The irradiance of the lamp used was 29.2 mW/cm<sup>2</sup> as stated previously in the Section 2. Fig. 1 showed the lamp irradiation wavelength domain between 320 and 800 nm. In the absence of CuO (upper trace) the *E. coli* bacteria increases with time, as expected.

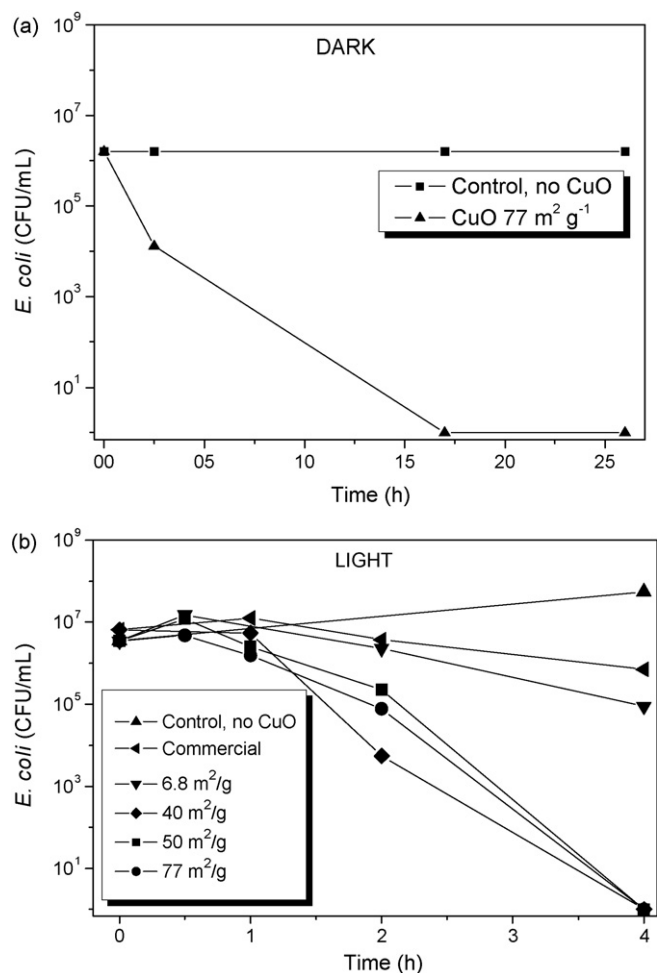
Fig. 3 shows the *E. coli* inactivation as a function of the amount of CuO powder (77  $m^2/g$ ) in solution under light irradiation at pH 7.1. Fig. 3 (upper trace, control experiment) shows that the solutions without CuO did not induce *E. coli* inactivation and that the *E. coli* grows only slightly within the reaction time. But solutions containing 0.1 and 1.0 g/L of CuO inactivate completely *E. coli* within 4 h. A higher amount of CuO (1.5 g/L) is able to complete the *E. coli* inactivation under light irradiation within 1 h. The solutions used were black suspensions, they absorb the incoming light within a few microns. We think that this is the case for the solutions in Fig. 3 with CuO added between 0.1 and 2.0 g/L.

Fig. 4 shows the effect of the light intensity on the *E. coli* inactivation time. It is readily seen that the light irradiation induced cell inactivation with  $\lambda > 360$  nm without a grey filter (29.2 mW/cm<sup>2</sup>). A grey filter reducing the incident light by a factor of two lead to *E. coli* inactivation with similar kinetics showing that a reduction by a factor of two in the incident light intensity did not slow the *E. coli* inactivation process. Fig. 4 also shows that a 12 times reduction in the incident light severely hinders the *E. coli* abatement and only a decrease in *E. coli* from  $10^7$  to  $10^5$  CFU/mL within 4 h was possible.

The *E. coli* recovery after light exposure was investigated following the post-irradiation effects in the following way: a solution containing *E. coli* was irradiated for 1 h 30 min and 2 h, respectively. The inactivation of *E. coli* was followed during the dark post-irradiation period and measured up to 8 h (Fig. 5). When light was applied during 1 h 30 min the CuO [4] seems to produce enough oxidative radicals leading to *E. coli* viability up to 8 h. A decrease of the bacterial population in the dark after initial illumination is feasible with the consequent savings in electrical energy. When light was applied for 2 h, the “residual effect” in the dark due to the radicals in solution was more severe and microbial count concentration decreased to the detection limit, in this case 1 CFU/0.4 mL = 2.5 CFU/mL.

#### 3.2. Copper speciation as a function of time in the presence of *E. coli*

Fig. 6 shows the  $Cu^{1+}$  generated in solution under light within the reaction time. The  $Cu^{1+}$ -ions entering the solution are seen to



**Fig. 2.** (a) Inactivation of *E. coli* as a function of time in the dark and in the presence of CuO (77  $m^2/g$ ) added to the solution in a concentration of 1 g/L. (b) Inactivation of *E. coli* in solution in the presence of several CuO (1 g/L) powders with different specific surface areas at pH 7.1. Filter cutoff allows for light  $h\nu > 360$  nm.

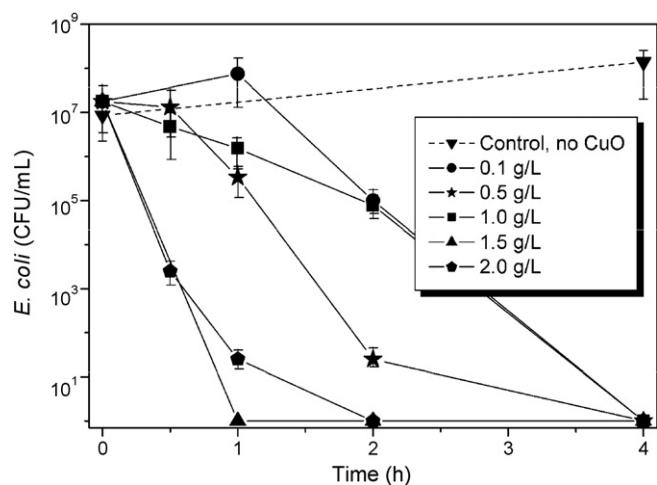


Fig. 3. Inactivation of *E. coli* as a function of the concentration of CuO (77 m<sup>2</sup>/g) under light irradiation >360 nm.

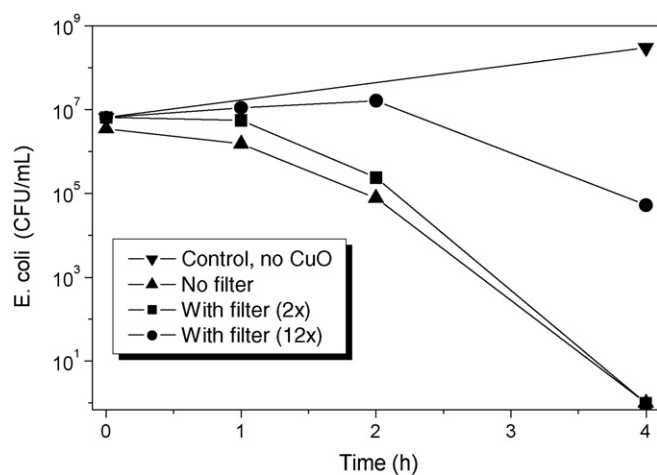


Fig. 4. Inactivation of *E. coli* with CuO (77 m<sup>2</sup>/g) in a concentration of 1 g/L under light irradiation with neutral filters cutting the incoming irradiation by 2 and 12 times. Control experiment without filter blocking the light <360 nm.

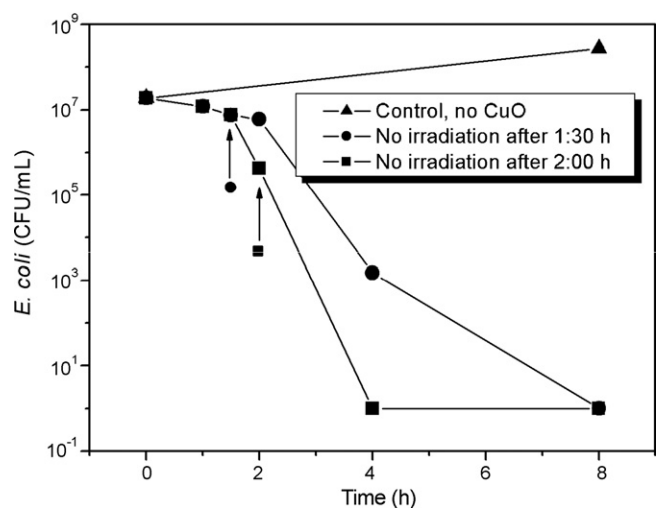


Fig. 5. Inactivation of *E. coli* in solution of CuO (77 m<sup>2</sup>/g, 1 g/L) applying the light source for 1 h 30 min or 2 h as shown by the arrows after the illumination periods. Bacterial inactivation is shown during the post-irradiation period.

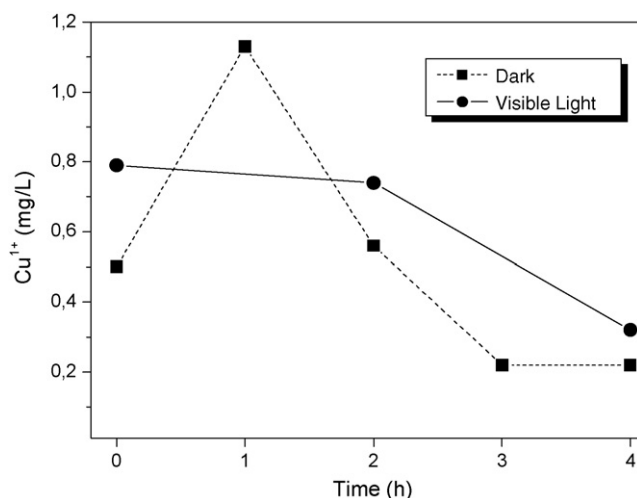


Fig. 6. Change of the concentration of Cu(I) during irradiation of a solution of CuO (77 m<sup>2</sup>/g), 1 g/L at pH 7.1.

rejoin the CuO matrix again in about 4 h due to the overwhelming presence of CuO in the suspension and undergoing re-oxidation to join the Cu(II)O state of the crystal lattice. The details of this type of self-cleaning mechanism in nature involving cations entering aqueous solutions and being re-adsorbed in the crystal lattice have been reported before [4]. Therefore, light irradiation may induce redox cycles Cu(I)/Cu(II). The decrease in the Cu<sup>1+</sup> reported in Fig. 6 occurs concomitantly to the *E. coli* inactivation time of 4 h (see Fig. 2b through Fig. 5).

### 3.3. H<sub>2</sub>O<sub>2</sub> determination in the presence and in the absence of *E. coli*

The traces showing the H<sub>2</sub>O<sub>2</sub> generated in solution in the absence of *E. coli* in the dark and under light (Fig. 7) show a trend similar to the traces reported in Fig. 6 for the production of Cu<sup>1+</sup> in solution. The higher H<sub>2</sub>O<sub>2</sub> production in the upper two traces in Fig. 7 is due to the sacrificial role of the *E. coli* acting as electron donors during the H<sub>2</sub>O<sub>2</sub> generation process. The production of H<sub>2</sub>O<sub>2</sub> increases as long as the bacteria is still present in the solu-

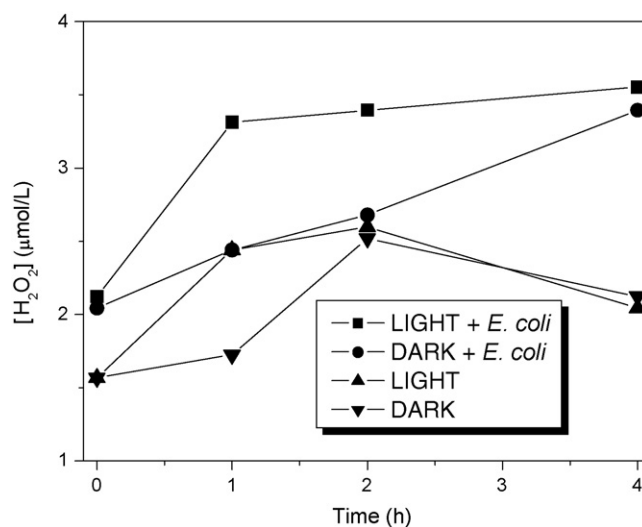
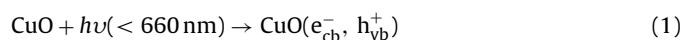


Fig. 7. Variation in the concentration of H<sub>2</sub>O<sub>2</sub> in solutions in the dark and under light irradiation (λ > 360 nm). The make up of the solution is: 1 g/L CuO of 50 m<sup>2</sup>/g and the solutions contain in the upper 2 traces of *E. coli* 10<sup>7</sup> CFU/mL.

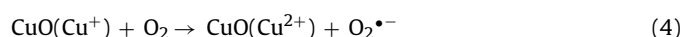
tion. The bacteriostatic action of Cu-ions in the dark in Fig. 7 has been ascribed to the capacity of Cu-ions to enhance the displacement reactions, disrupt enzyme structures and binding thiols on proteins [19,20]. In this case H<sub>2</sub>O<sub>2</sub> would play a minor role in *E. coli* inactivation. The generation of H<sub>2</sub>O<sub>2</sub> may involve complicated processes with several intermediate steps. This is reflected by the trends of the traces in Fig. 7.

### 3.4. Suggested mechanism of reaction at the CuO under light irradiation

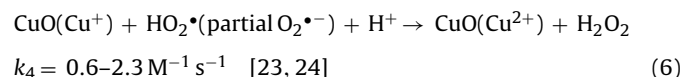
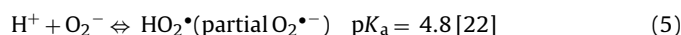
Fig. 2b shows that up to 2 h under light irradiation the outer membranes of *E. coli* resist the effects of CuO mediated inactivation fairly well. A resistance by the cell membrane to the reactive radical species (or ROS) [18,19] is observed within 1–2 h of reaction. After 2 h reaction a steeper decrease in cell inactivation is observed as it has been reported previously. The same trend has been reported when using other semiconductors active in bacterial immobilization [19]. The semiconductor character of CuO has been described [3,4,6,21]. Under CuO irradiation leads steps to oxidative radicals by a mechanism that is suggested below from Eq. (1) on



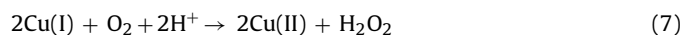
The  $e_{\text{cb}}^-$  in Eq. (1) is produced from the CuO (p-type) with a band gap energy of 1.7 eV, a flat-band potential of  $-0.3 \text{ V SCE}$  (pH 7) and a valence band at  $+1.4 \text{ V SCE}$  [21]. The electron-hole pair is formed with photon energies exceeding the band gap of CuO. The excited electron could either react (a) directly with the O<sub>2</sub> forming O<sub>2</sub><sup>•-</sup> (reaction (2)) or by (b) reducing the Cu<sup>2+</sup>-lattice to Cu<sup>+</sup> leading to the ensuing reactions (3)–(4) with formation of O<sub>2</sub><sup>•-</sup> radicals



Eq. (5) shows the equilibrium between H<sup>+</sup> and O<sub>2</sub><sup>•-</sup> leads to the formation of the HO<sub>2</sub><sup>•</sup> radical. The HO<sub>2</sub><sup>•</sup> stated in Eq. (5) and leads to the production of H<sub>2</sub>O<sub>2</sub> in Eq. (6)



or the alternative reaction:



Eq. (6) is analogous to the behavior of Fe<sup>2+</sup>-ions (Fenton reaction) in the Haber–Weiss cycle [25]. Indeed, the production of H<sub>2</sub>O<sub>2</sub> as expected in Eq. (7) was evaluated experimentally in both dark and illuminated culture medium and in the presence and in the absence of bacterial cells (see Fig. 7). The hydrogen peroxide production was observed to be always higher than the sample kept in the dark in the presence and in the absence of *E. coli* at the beginning of the experiment, but show similar values after 4 h reaction. This behavior was observed both in the presence and in the absence of *E. coli*, although higher levels of H<sub>2</sub>O<sub>2</sub> were measured in the culture medium containing *E. coli*. Considering the background levels of H<sub>2</sub>O<sub>2</sub> in natural waters to be around 0.4 μmol/L [25,26] one can expect H<sub>2</sub>O<sub>2</sub> production using CuO at least 4 times higher, reaching values from 1.5 to 3.5 μmol/L. Recently, it has been reported that H<sub>2</sub>O<sub>2</sub> in rain water could reach values as high as 30 μmol/L [27]. It is not clear, however, if hydrogen peroxide concentrations in the order of few μmol/L as the one measured in these experiments could be the

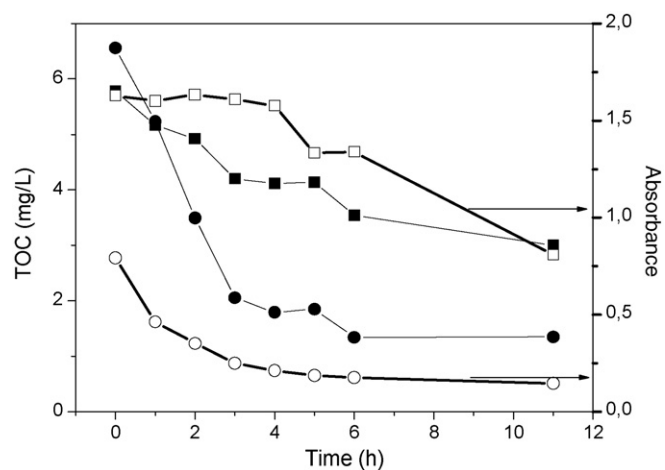


Fig. 8. Dye absorbance (right axis and open symbols) for methylene blue (MB, squares) measured at 665 nm, and Orange II (circles) measured at 476 nm illuminated with irradiation  $\lambda > 360 \text{ nm}$ . Solution pH 7.1; CuO (1 g/L). Full symbols show the TOC variation for (solution pH 7.1; CuO (1 g/L). Full symbols show the TOC variation for both dyes left axis).

major responsible for the inactivation of *E. coli*, as the formation of other highly oxidative transient species such as superoxide (see above reactions (5) and (6)) cannot be ruled out. A similar mechanism involving Cu(I), Cu(II) and naturally occurring organic matter leading to the generation of superoxide radicals in photo-induced processes in natural waters has been proposed by Jardim et al. [28].

In our case we suggest that, the Cu(I)-ions on the CuO is the active catalytic species in accordance to Eq. (8) below.



The oxidative side of the redox cycle would involve the  $h^+$  in Eq. (2) and converts the H<sub>2</sub>O into OH-radicals allowing for the hole transfer and the later species leads to the formation of H<sub>2</sub>O<sub>2</sub> in Eq. (10).



The above mechanism for copper toxicity implies the capacity of CuO to generate reactive oxygen species (ROS) involving Cu-ions via Fenton-like reactions through the Haber–Weiss [29] cycle. The inhibition of the *E. coli* enzymatic activity is also caused due to the Cu-ion binding of the *E. coli* cell walls thiol proteins [30] since Cu<sup>1+</sup> has been reported to have the ability to bind indiscriminately to cell walls [31]. This last property (inhibition of enzymatic activity as shown by the overall trends observed in Figs. 2–5) is related to the profile of Cu<sup>1+</sup> generation in solution shown in Fig. 6.

### 3.5. Photodegradation of dyes mediated by CuO under visible light

Fig. 8 shows the degradation of Orange II and methylene blue mediated by CuO under light with  $\lambda > 360 \text{ nm}$ . These experimental results show that the CuO is able not only to inactivate bacteria but also to oxidize dyes having bonds with a higher strength compared to the ones found in living matter. The degradation mediated by TiO<sub>2</sub> under UV light of these two dyes has been widely reported in the literature involving electron transfer from the TiO<sub>2</sub> $e_{\text{cb}}^-$  [6]. The CuO efficiently transfers its conduction band electron into the aqueous solution due to its metallic character.

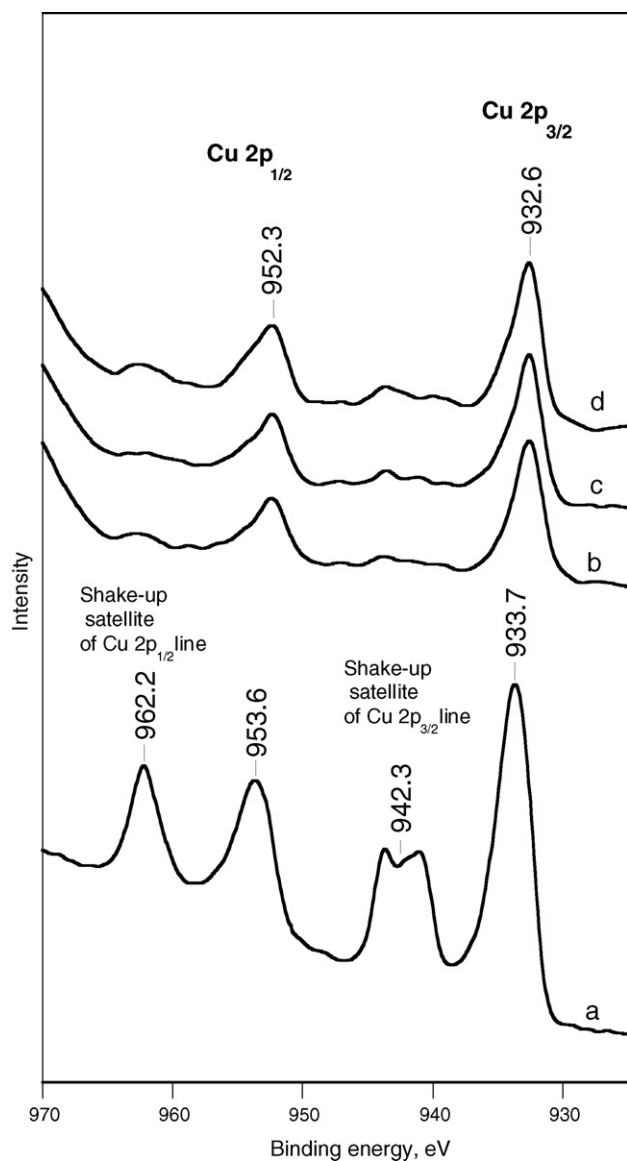


**Fig. 9.** XPS Cu 2p line (doublet plus two shake-up lines for CuO): (a) fresh catalyst, and after different contact times with suspension of bacteria, (b) immediately after contact with catalyst, (c) after contact with catalyst for 1 h and (d) after contact with catalyst for 4 h.

### 3.6. XPS studies of the CuO catalyst surface during *E. coli* inactivation

The atomic surface concentration of copper catalyst directly after preparation and after contact (in the dark) with the *E. coli* bacterial suspension in a buffer solution are presented in Table 1 below.

The XPS experiments give information about the outermost surface layer of the CuO catalyst in range of ~5–7 nm. These outer layers are the most important part of catalyst determining its properties and activity and show often a composition different from that in bulk. When the CuO is exposed to the bacterial suspension, their surface is covered by adsorbed bacteria. This leads to a lower intensity of the copper signal as reported in Table 1. Also Na, K, P, and S elements were detected on the catalyst surface as adsorbed ions. These elements come from the buffer solution used to prepare the *E. coli* suspensions to regulate the pH in the bacterial solution (see Section 2).

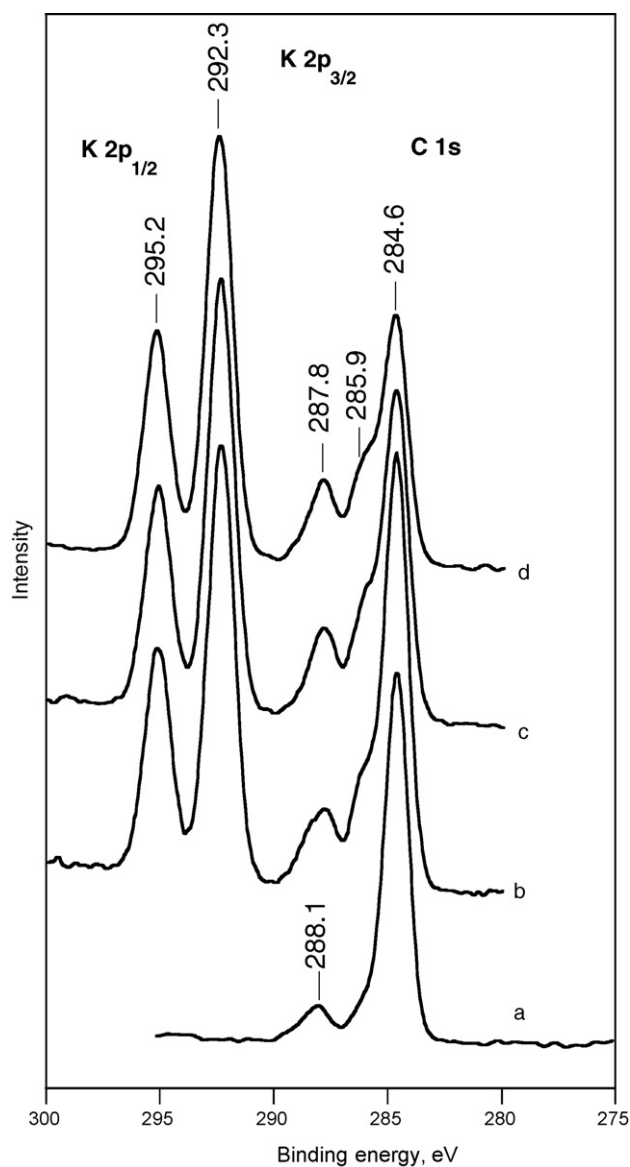


**Fig. 10.** XPS C 1s and K 2p lines: (a) fresh catalyst (absence of K 2p line), and after different contact times with bacterial suspension, (b) immediately after contact with catalyst, (c) after contact with catalyst for 1 h and (d) after contact with catalyst for 4 h.

The major XPS results are presented in Figs. 9 and 10. The spectra of the CuO recorded immediately after preparation indicate that the catalyst contains mainly CuO with small surface amounts of CuCO<sub>3</sub> and Cu(OH)<sub>2</sub>. The Cu 2p<sub>3/2</sub> and Cu 2p<sub>1/2</sub> lines positioned at 933.7 and 953.6 eV, respectively and shake-up satellite lines of Cu 2p at 942.3 and 962.2 eV (Fig. 9) indicate the presence of Cu<sup>2+</sup> paramagnetic species. The O 1s line at 531.2 eV (not shown in Fig. 9) and C 1s line at 288.1 eV in Fig. 10 indicate the presence of surface OH<sup>-</sup> and CO<sub>3</sub><sup>2-</sup> copper species.

After the CuO is contacted with the bacterial suspension prepared in buffered solutions, some remarkable spectral changes were observed as shown below in the text in Figs. 9 and 10, and Table 1. An important observation is that the surface of CuO exposed to bacterial suspension almost completely changes its oxidation state from Cu<sup>2+</sup> to Cu<sup>+</sup>. Decomposition of the Cu 2p<sub>3/2</sub> line reveals that the outermost layer of the catalyst becomes 80% in Cu<sub>2</sub>O and only 20% remains as CuO. The evidence for this observation is the shift in the Cu 2p<sub>3/2</sub> and Cu 2p<sub>1/2</sub> lines positioned initially at 933.7

and 953.6 eV to 932.6 and 952.6 eV, respectively for catalysts contacted with bacteria. Moreover, the concomitant disappearance of the  $\text{Cu}^{2+}$  shake-up satellite lines at 942.3 and 962.2 eV (Fig. 9) also indicates that the transformation of CuO to  $\text{Cu}_2\text{O}$  is taking place. Hence, the catalyst surface is almost immediately reduced after the CuO contacts the bacteria and remains in reduced state during the 4 h of reaction with the bacterial suspension.

The amount of the adsorbed bacteria could be determined from the observation of the intensity of C 1s line in Fig. 10. In the presence of light the intensity of the C 1s decreases several times within the reaction time up to  $t=4$  h. At the same time, signals due to the presence of the buffer components like P 2p, Na 1s (not shown) and K 2p in Fig. 10 show similar intensities for each element in the samples under study.

In summary, new evidence has been presented for the reduction of the CuO high surface area catalyst to  $\text{Cu}_2\text{O}$  with concomitant *E. coli*/immobilization/oxidation occurs. No accumulation of intermediate species at the catalyst surface was observed during the *E. coli* degradation that would hinder the CuO oxidation/reduction cycles taking place.

#### 4. Conclusions

This study shows: (a) that stable large specific surface area CuO photocatalysts were effective in the inactivation of *E. coli*, (b) that visible light induced CuO mediated *E. coli* immobilization proceeds with an acceptable kinetics at biological pH ( $\sim 7$ ) and faster than in dark processes, (c) that CuO suspensions activated by visible light were effective in photocatalyzing the degradation of anionic (Orange II) and cationic dyes (MB), (d) that only Cu-ions adsorbed on CuO seem to be effective during *E. coli* inactivation involving interfacial charge transfer processes, (e) that CuO shows a potential use as bactericide that could be used on suitable supports for external (skin related) applications in the medical field and finally (f) evidence was presented by XPS that the CuO surface is reduced to  $\text{Cu}_2\text{O}$  by contact with *E. coli* during the bacterial inactivation process.

#### Acknowledgements

We wish to thank the COST Action 540 Phonasum "Photocatalytic technologies and novel nano-surface materials, critical issues" for financial support.

#### References

- [1] D.K. Karlin, Y. Gulneth, In Progress in Inorganic Chemistry, vol. 35, Lippard, Ed., 1987, pp. 220–237.
- [2] B.W. Tolman, Acc. Chem. Res. 30 (1997) 227–240.
- [3] J. Bandara, I. Guasaquillo, P. Bowen, L. Soare, F.W. Jardim, J. Kiwi, Langmuir 21 (2005) 8554–8559.
- [4] J. Bandara, J. Kiwi, C. Pulgarin, P. Peringer, G.-M. Pajonk, A. Elalui, P. Albers, Environ. Sci. Technol. 30 (1996) 1261–1267.
- [5] D. Li, T. Yuranova, J. Kiwi, Water Res. 38 (2004) 3541–3550.
- [6] Th. Oppenlaender, Photochemical Purification of Water and Air, Wiley-VCH, Weinheim, Germany, 2003.
- [7] Y. Gak, V. Nadtochenko, J. Kiwi, J. Photochem. Photobiol. A. 116 (1998) 57–62.
- [8] L.C. Carnes, J. Stipp, J. Klabunde, J. Bonevich, Langmuir 18 (2002) 1352–1358.
- [9] W. Wang, X. Zhan, Y. Wang, Y. Liu, G. Zheng, G. Wang, Mater. Res. Bull. 37 (2002) 1092–1100.
- [10] A. Sadana, J. Katzer, J. Catal. 35 (1974) 140–152.
- [11] Th. Hai-Yan, C. Yu-Ling, L. Jing-Kui, X.J. Si-Shen, Mater. Sci. 28 (1993) 5176–5178.
- [12] D. Walsh, T. Arcelli, J. Ikoma, J. Tanaka, S. Mann, Nat. Mater. 2 (2003) 386–388.
- [13] T. Yokota, Y. Kubota, Y. Takahata, T. Katsuyama, Y. Matsuda, J. Chem. Eng. Jpn 37 (2004) 238–244.
- [14] G. Anon, Drug Ther. Bull. 40 (2002) 67–69.
- [15] H. Bader, V. Sturzenegger, Hoigné, J. Wat. Res. 22 (1988) 1109–1115.
- [16] A. Hulanicki, T.K.V. Krawczyk, A. Lewenstam, Anal. Chim. Acta 158 (1984) 343–355.
- [17] P.R. Murray, E.J. Baron, M.A. Pfaller, F.C. Tenover, R.H. Tenover, Manual of Clinical Microbiology, sixth edition, American Society of Microbiology, Washington, D.C., 1995.
- [18] T.E. Cooney, Infect. Control. Hosp. Epidemiol. 16 (1995) 444–450.
- [19] R. Bacsá, J. Kiwi, T. Ohno, P. Albers, V. Nadtochenko, J. Phys. Chem. B. 109 (2005) 5994–6003 (and references therein).
- [20] K. Sunada, T. Watanabe, K. Hashimoto, Environ. Sci. Technol. 37 (2003) 4785–4789.
- [21] K. Hardee, A. Bard, J. Electrochem. Soc. 124 (1977) 215.
- [22] K. Hardee, A. Bard, J. Electrochem. Soc. 124 (1977) 215–224.
- [23] S. Goldstein, G. Czapski, D. Meyerstein, J. Am. Chem. Soc. 112 (1990) 6489–6493.
- [24] J.B. Bielski, D. Cabelli, R. Arudi, A. Ross, J. Phys. Chem. Ref. Data 14 (1985) 1041–1061.
- [25] R.G. Petasne, R.G. Zika, Mar. Chem. 56 (1997) 215–225.
- [26] R.J. Kieber, R.H. George, Estuarine, Coastal Shelf Sci. 40 (1995) 495–9503.
- [27] W.J. Cooper, D.R.S. Lean, Environ. Sci. Technol. 23 (1989) 1425–1428.
- [28] W.F. Jardim, M.I. Soldá, S.M. Gimenez, Sci. Total Environ. 58 (1986) 47–54.
- [29] J. Weiss, Naturwissenschaften 23 (1935) 64–67.
- [30] M.E. Letelier, A. Lepe, M. Faundez, J. Salazar, R. Marin, P. Aracena, H. Speisky, Chem.-Biol. Interact. 151 (2005) 71–82.
- [31] N. Takeshi, M. Insook, S. Noriyuki, I. Takakiro, J. Biol. Chem. 272 (1997) 23037–23041.